JMEPEG (1996) 5:446-451

Amorphous Superconducting Transformation in Bismuth-Base High-T_c Superconducting Rods

M.N. Khan and A. Ul Haq

The transformation of high-resistivity amorphous $(Bi_{1.68}Pb_{0.32})Sr_{1.75}Ca_{1.85}Cu_{2.85}O_y$ and $(Bi_{1.6}Pb_{0.4})Sr_{1.7}Ca_{2.3}Cu_3O_y$ to superconductive materials has been characterized by structural, thermochemical, transport, and scanning electron microscope measurements. X-ray powder diffraction confirmed that rapid solidification of Bi-Pb-Sr-Ca-Cu-O_y yields amorphous material. In further heat treatments, sequential crystallization of three phases was identified.

Differential scanning calorimetry indicated an exothermic crystallization peak at 520 °C with corresponding enthalpy of 62 J/g. Scanning electron microscopy studies revealed that the grain size increases with sintering time and that the formation mechanism in the interior of the bulk is different from that at the surface of the superconducting glass ceramic rods. Thermal cycling of the insulating glass to a temperature above that required for crystallization results in a transformation from an insulating to a superconducting material with a T_c (R = 0) of 105 K. It was also shown that the glass ceramic rods obtained by reheating glass rods to 850 °C for 120 h have a T_c (R = 0) of 105 K, whereas the disk specimens obtained by reheating the powdered glass compacts in the same way do not exhibit superconductivity above 85 K. This difference in superconductivity between the specimens is discussed in terms of the crystallization process and the amount of oxygen absorption of the specimens during heating.

Keywords

amorphous, enthalpy, kinetics, microstructure, transformation

1. Introduction

THE DISCOVERY of glass formation in the system Bi-(Pb)-Sr-Ca-Cu-O (Ref 1-3) has encouraged the fabrication of high-T_c superconductor fibers via glass precursors. Research has also concentrated on isolating the high-T_c phase using conventional ceramic processing techniques. It has been reported that the superconducting transition temperature of the system is closely related to the layered crystal structure of the unit cell. Early results (Ref 4) showed that the compound $Bi_2Sr_2CuO_4$ with only one Cu-O plane in the unit cell has T_c values less than 20 K.

The 80 K superconducting phase has been identified to have a composition of $Bi_2Sr_2Ca_1Cu_2O_x$ (Ref 5, 6); two Cu-O planes in the unit cell have been observed with high-resolution lattice imaging. The composition responsible for the 110 K is controversial; however, the reported possible composition is $Bi_2Sr_2Ca_2Cu_3O_x$, with three Cu-O planes in the unit cell (Ref 6, 7). The formation of the 110 K phase has been found to be associated with the composition of the starting material for sintered bulk polycrystalline samples. The sintering condition and subsequent heat treatment also play important roles in obtaining the high-T_c superconducting phase. The kinetics of 2223* phase formation are controlled by calcium and copper diffusion. The presence of lead accelerates the growth of the 2223 phase by enhancing diffusion of calcium and copper during insertion of an extra layer of Ca-O and Cu-O into the unit cell of 2212**. The lead atoms are incorporated into the structure probably because bismuth in the +3 oxidation state and lead in the +2 state have the same outer electronic shell configuration of $6S^26P^0$. On the other hand, substitution of the higher Pb^+ cation (ionic radius = 1.20 Å for Bi^{3+} (ionic radius = 0.96 Å) probably results in distortion of the crystal lattice.

Differential scanning calorimetry (DSC) and differential thermal analysis (DTA) are versatile thermoanalytical techniques for studying the kinetics of phase transformations and other processes. Various mathematical analyses on nonisothermal solid-state transformations from DSC and DTA measurements have been reported (Ref 8). Drawing glass fibers from the melt is a well-established technique in the glass industry and can also be employed for fabrication of the high-temperature super conductors (HTS) fibers. Before this can actually be done, however, it is desirable to understand glass formation in the superconducting oxide systems and crystallization of the superconducting phase(s) in the resulting glasses on thermal treatment.

We prepared the $(Bi_{1.68}Pb_{0.32})Sr_{1.75}Ca_{1.85}Cu_{2.85}O_y$ and $(Bi_{1.6}Pb_{0.4})Sr_{1.7}Ca_{2.3}Cu_3O_y$ composition*** material for amorphous-to-crystalline phase transformations. We also investigated mechanisms, microstructures, phase development, and resistivity measurements of $(Bi_{0.68}Pb_{0.32})Ca_{1.85}Sr_{1.75}Cu_{2.85}O_y$ and $(Bi_{1.6}Pb_{0.4})Sr_{1.7}Ca_{2.3}Cu_3O_y$ superconductors.

2. Experimental Procedure

Appropriate amounts of Bi_2O_3, $SrCO_3$, CaCO (99.95% STREM Chemical Company), and CuO for the nominal compositions $(Bi_{1.68}Pb_{0.32})Sr_{1.75}Ca_{1.85}Cu_{2.85}O_y$ and $(Bi_{1.6}Pb_{0.4})Sr_{1.7}Ca_{2.3}Cu_3O_y$ were slurry mixed in acetone and ground using a mortar and pestle. The mixture was calcined in an alumina crucible in air at 795 °C overnight, cooled, and re-

M.N. Khan, High Temperature Superconductivity Laboratory, Department of Physics, University of Bahrain, P.O. Box 32038; Bahrain; and **A. Ul Haq,** Metallurgy Division, Dr. A.Q. Khan Research Laboratories, Kahuta, P.O. Box 502, Rawalpindi, Pakistan.

*2223 is shorthand for $Bi_2Sr_2Ca_2Cu_3O_y$.

**2212 is shorthand for $Bi_2Sr_2Ca_1Cu_2O_y$.

***The overall compositions are expressed in terms of chemical stoichiometric formulas.

ground. The pulverized gray powder was melted in a covered platinum crucible in an electric furnace at 1250 °C for 0.5 h. The melt was rapidly quenched by pressing between two copper plates, resulting in opaque black sheets of glass 1 mm thick (specimen A) that were found to be amorphous.

From the same crucible the melts were pumped up into fused silica tubes (≈2 mm diam), resulting in the formation of crystal-free glassy rod specimens. The inner glass rods (specimen B) were removed mechanically from the outer silica tubes for the subsequent experiment.

Another specimen (C) was prepared from powdered sample B. First, sample glass B was prepared, then pulverized into fine powder (0.5 to 4 μm diam); next, a disk (≈20 mm diam by 2 mm thick) was made by pressing (4 MPa). For the heat treatment, the glassy rod specimen B (≈2 mm diam) was cut into 20 mm long pieces, and the powder-compacted glassy specimen C was cut into rectangular bars (≈2 × 4 mm^2 by 15 mm).

All three specimens (A, B, and C) were placed on an alumina plate and reheated in air at a heating rate of 2 °C/min to a given temperature (840 to 850 °C) at which they were held for 50 h to crystallize. Then they were cooled to room temperature in the furnace.

X-ray diffraction (XRD) patterns were recorded with CuK_α radiation in the 2θ range of 10° to 62° using an automated diffractometer.

Thermogravimetric and DSC analyses were performed on as-quenched fragments to determine the crystallization and glass transition temperatures, using a Setaram TMA 92 (Caluire Cedex, France) interfaced with a computerized data analysis system. Resistivity versus temperature measurements were made by a common four-probe technique.

For scanning electron microscope (SEM) measurements, a glass rod was cut in 6 to 7 mm long pieces. Four were embedded in an epoxy for metallographic investigations. After embedding, one of the pieces was sectioned again in order to examine the interior structure. The sample was then coated with carbon to perform further investigations using an SEM equipped with EDX (energy-dispersive x-ray analysis).

3. Results and Discussion

Figure 1 shows the XRD patterns of $(Bi_{0.68}Pb_{0.32})Sr_{1.75}Ca_{1.85}Cu_{2.85}O_y$ sample annealed at 850 °C for different lengths of time. Various phases present in the crystallized samples were identified from the diffraction patterns. All the samples were seen to be multiphase. On heating the glass, $Bi_2Sr_2Ca_0Cu_1O_6$(2201) phase crystallized out first, followed by formation of $Bi_2Sr_2Ca_1Cu_2O_8$ (2212) phase (T_c = 80 K). The 110 K T_c phase, probably $Bi_2Sr_2Ca_2Cu_3O_{10}$ (2223), began appearing in samples by reaction between the phases formed at lower temperatures. The fraction of the 2223 phase increased with the time of annealing at 850 °C.

As shown in Fig. 1, prolonged heating at 850 °C (from 6 to 10 days) did not significantly influence the phase changes. One explanation is that for the 2223 composition, the crystallized glass had reached thermodynamic equilibrium state by 6 days, in which the 85 and 110 K phases coexist. It should be noted that when several 2223 samples were annealed at 850 °C for less than 4 days, no resistive drops at 105 K were observed.

It is interesting to note that the phase changes were still quite rapid when annealed at different lengths of time. As can be seen in Fig. 1(b), the two peaks appearing at 2θ = 35.3° and 35.7° when the sample was annealed at 850 °C for 50 h became a single 110 K phase peak at 35.5° (Fig. 1d), when the sample was annealed at 850 °C for 6 days.

Based on the results of this research, it appears that formation of the 110 K phase requires thermally activated, long-range diffusion at the higher temperature range (>850 °C). X-ray diffraction analysis also revealed that the structure of these materials annealed at 850 °C for more than 120 h was strongly anisotropic (a = 3.8 Å and c = 37 Å).

Figure 2 shows the XRD patterns at room temperature for the melt-quenched and annealed samples of $(Bi_{1.6}Pb_{0.4})Sr_{1.7}Ca_{2.3}Cu_3O_y$ polycrystalline material. X-ray diffraction analysis data showed that the structure of these materials annealed at 850 °C for 140 h was also strongly anisotropic (a = 4.38 Å and c = 38 Å).

The amorphous structure of the preannealed sample was confirmed by powder XRD analysis (Fig. 1a). The diffraction pattern of the glass showed only a diffuse maxima centered at about 2θ = 30°.

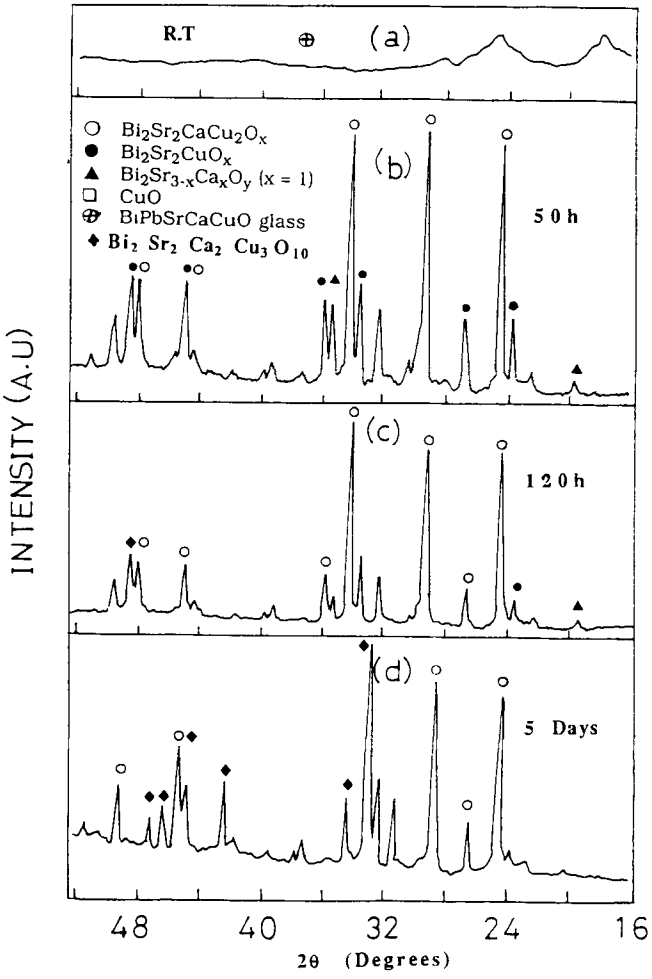

Fig. 1 XRD patterns at room temperature for $(Bi_{1.68}Pb_{0.32})Sr_{1.75}Ca_{1.85}Cu_{2.85}O_y$ sample annealed at 850 °C for different lengths of time

Figure 3 shows the T_c (zero) values and the relative XRD peak intensities of the 110 K phase plotted against the heat treatment temperature. The relative XRD peak intensities were calculated from $I_{108\ K\ (0.002)}/I_{80\ K\ (002)}$, where $I_{108\ K\ (0.002)}$ and $I_{80\ K\ (002)}$ are the intensities of the XRD peaks due to the diffraction from the (002) plane of the 108 K phase and of the 80 K phase, respectively. The T_c values, which range from 85 to 108 K, were maximized when the heat treatment was performed at 855 °C. The relative peak intensities of 108 K phase were also maximized at around 850 to 856 °C.

The DTA curve (Fig. 4) of the polycrystalline material showed that the glass transition temperature was about 494 °C and that the crystallization temperature was 520 °C. The liquid temperature of the glass was about 860 °C. A typical DSC scan of $(Bi_{1.6}Pb_{0.4})Sr_{1.7}Ca_{2.3}Cu_3O_y$ glass showing the glass transition (T_g) and crystallization (T_x) temperatures is depicted in Fig. 5. The T_g and T_x temperatures for this system are 380 and 463 °C, respectively. Several other exothermic and endothermic peaks are also observed at temperatures above T_x. The thermogravimetry (T_G) curve in air for the bulk sample is also shown in Fig. 5. The weight gain begins around 700 °C, and the maximum gain occurs at about 813 °C. These results indicate that the diffusion of oxygen into the interior of the sample and at temperatures below around 600 °C was very slow.

We note that the endothermic peak appears at 799.8 °C in the bulk sample. It is of particular interest to clarify the origin of this endothermic peak, because the $Bi_2Sr_2Ca_2Cu_3O_x$ phase precipitates and grows above this endothermic temperature. It is clear that the reaction among the $Bi_2Sr_{3-x}Ca_xO_y$ ($x = 1$), CuO, and $Bi_2Sr_2CuO_x$ phases in the interior of the sample is closely related at around 799.8 °C. We summarize the crystallization mechanism as follows: The 2201 phase first precipitates out, followed by formation of 2212 phase at higher temperatures. The 110 K T_c phase is formed at 861.5 °C just below the melting point, probably by reaction between the low-T_c 2201 and 2212 phases and the residual calcium and copper oxides.

Figure 6 presents a typical DTA curve for the rod $(Bi_{1.6}Pb_{0.4})Sr_{1.7}Ca_{2.3}Cu_3O_y$, showing exothermic and endothermic peaks corresponding to different phases.

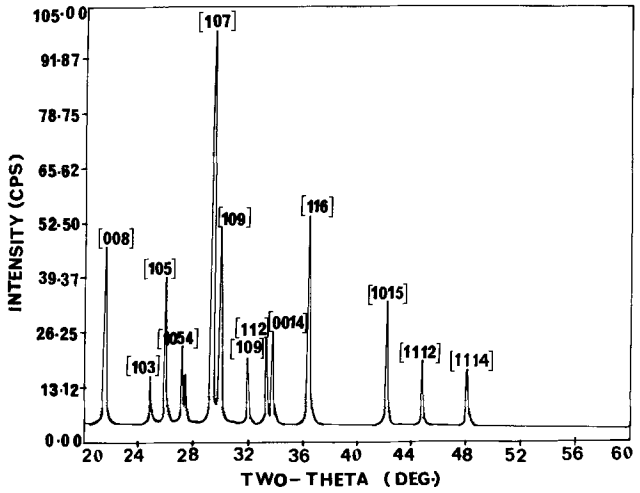

Fig. 2 XRD patterns at room temperature for $(Bi_{1.6}Pb_{0.4})Sr_{1.7}Ca_{2.3}Cu_3O_y$ sample annealed at 850 °C for 140 h

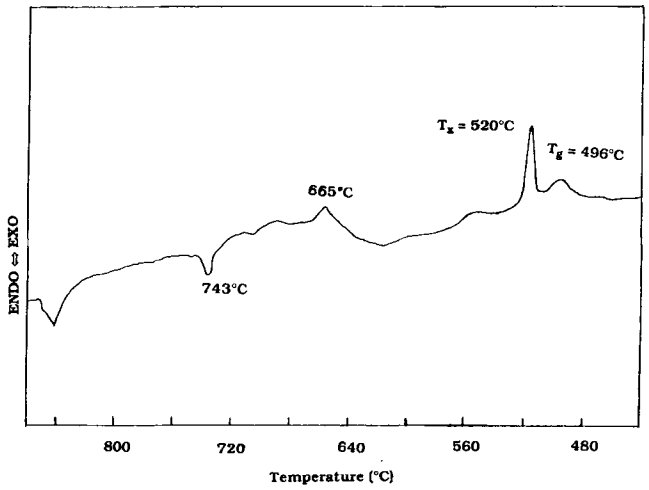

Fig. 4 DTA curve of $(Bi_{1.68}Pb_{0.32})Sr_{1.75}Ca_{1.85}Cu_{2.85}O_y$ glasses melted at 1250 °C

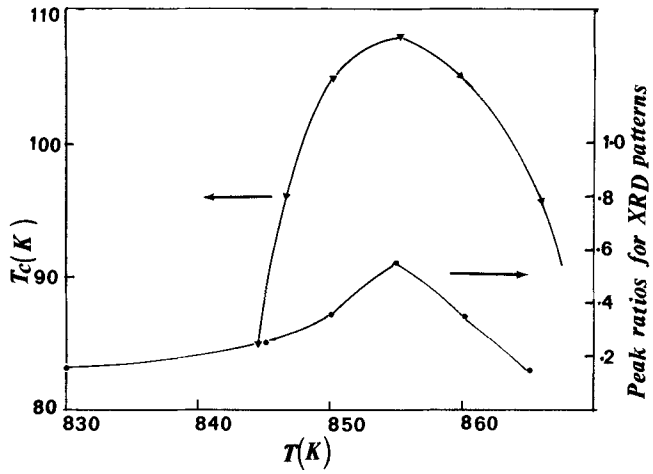

Fig. 3 T_c (zero) values and relative intensities of the 110 K phase peak (002) for $(Bi_{1.6}Pb_{0.4})Sr_{1.7}Ca_{2.3}Cu_3O_y$ samples plotted against the heat treatment temperature

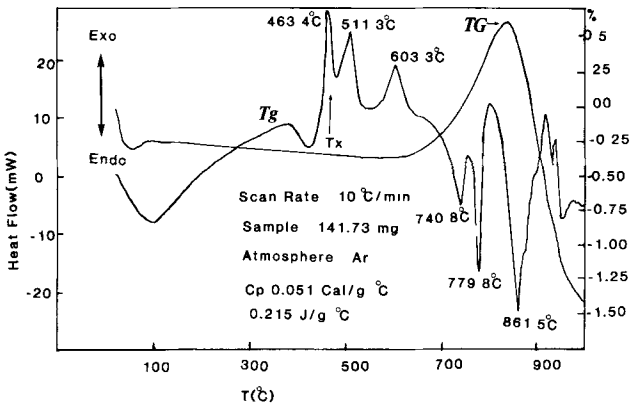

Fig. 5 Typical DSC scan of $(Bi_{1.6}Pb_{0.4})Sr_{1.7}Ca_{2.3}Cu_3O_y$ glass in argon atmosphere at a heating rate of 10 °C/min

Figure 7(a) shows the resistivity of the glass-rod ceramic as a function of temperature. It is found that the glass-rod ceramic specimens obtained after annealing for more than 120 h at 850 °C showed superconductivity with T_c ($R = 0$) of 105 K. In contrast, powder-crystallized specimen (Fig. 7b) obtained by the same heating schedule showed T_c ($R = 0$) at about 85 K. No significant difference in the crystalline phases was detected in these specimens, although the amount of oxygen absorption during heating of the two specimens is thought to be different. It could be concluded that the difference in superconducting properties for both specimens is primarily caused by the difference in the amount of oxygen absorption of the specimens during heat treatment.

Devitrification of Bi-Sr-Ca-Cu-O glasses is a serious problem during fiber drawing by heating a glass preform to around its softening point. Thus, knowledge of the crystallization kinetics of these glasses is a prerequisite for successful drawing of the glass fibers.

The theory of transformation kinetics (Ref 8) describes the evolution with time, t, of the volume fraction crystallized, x, in terms of nucleation frequency per unit volume, I_v, and the crystal growth rate, u:

$$x = 1 - \exp\left[-g\int_0^t I_v\left(\int_{t'}^t u d\tau\right)^m dt'\right] \quad \text{(Eq 1)}$$

Here g is a geometric factor that depends on the shape of the growing crystal, and m is an integer or half-integer that depends on the mechanism of growth and the dimensionality of the crystal.

For the important case of isothermal crystallization with nucleation rate and growth rate independent of time, Eq 1 can be integrated to yield:

$$x = 1 - \exp(-g' I_v u^m t^n) \quad \text{(Eq 2)}$$

where $n = m + 1$ for $I_v \neq 0$, and g' is a new shape factor.

Equation 2 can be expressed in terms of isothermal crystallization of a glass as a specific cast of the Johnson-Mehl-Avrami relation (Ref 9):

$$x = 1 - \exp[(-Kt)^n]$$

where x is the volume fraction crystallized after time t; n is the Avramic parameter, which depends on the crystal growth morphology; and K is the crystallization rate constant, whose temperature dependence (within the narrow temperature ranges) can be given by the Arrhenius equation:

$$K = \beta \exp\left[\frac{-E_a}{RT}\right] \quad \text{(Eq 3)}$$

where β is the frequency factor, E_a is the activation energy, R is the gas constant, and T is the isothermal absolute temperature.

Taking the logarithm of Eq 2 and rearranging gives:

$$-\ln(1 - x) = (Kt)^n \quad \text{(Eq 4)}$$

$$\ln[-\ln(1 - x)] = n \ln K + n \ln t$$

Isothermal DSC curves for crystallization of the glass were recorded at various heating rates for the crystallization of a glass. Values of kinetic parameters were calculated using the kinetic model (Ref 10), which is expressed as:

$$\ln\left[\frac{T_p^2}{\alpha}\right] = \ln\left(\frac{E_a}{R}\right) - \ln\beta + \frac{E_a}{(RT_p)} \quad \text{(Eq 5)}$$

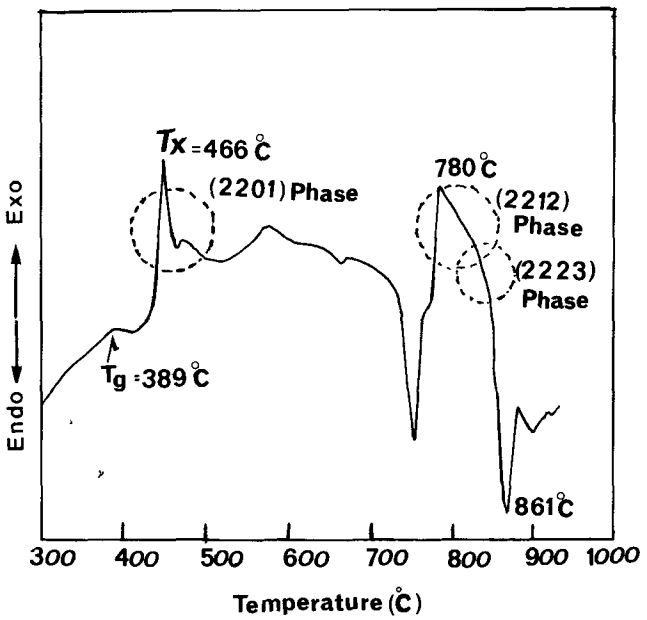

Fig. 6 DTA curve of $(Bi_{1.6}Pb_{0.4})Sr_{1.7}Ca_{2.3}Cu_3O_y$ glass melted at 1250 °C in air

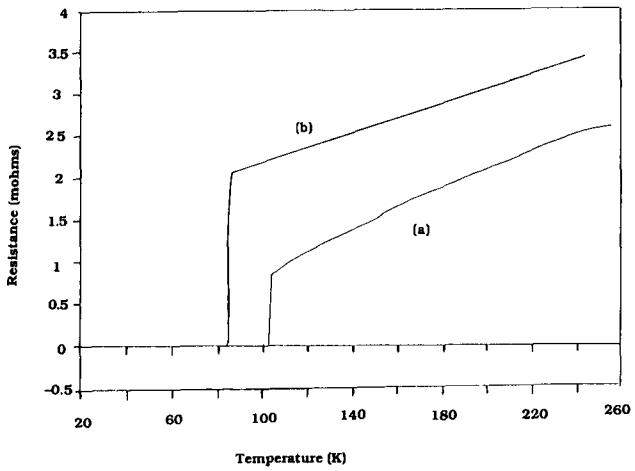

Fig. 7 Temperature dependence of resistance. (a) $(Bi_{1.68}Pb_{0.32})Sr_{1.75}Ca_{1.85}Cu_{2.85}O_y$ glass rod. (b) $(Bi_{1.68}Pb_{0.32})Sr_{1.75}Ca_{1.85}Cu_{2.85}O_y$ powder-compacted sample

where T_p is the peak maximum temperature in the DSC, and α is the heating rate. In the derivation of Eq 1, it has been assumed that the rate of reaction is maximum at the peak, which is valid for power-compensated DSC. For each of the four peaks observed in the DSC traces, peak temperatures were determined and the plot of $\ln(T_p^2/\alpha)$ versus $1/T_p$ for crystallization of the glass was linear (Fig. 8), indicating the applicability of the kinetic model. From linear least-squares fitting of the data, values of E_a for the crystallization of the glasses in the system $(Bi_{1.6}Pb_{0.4})Sr_{1.7}Ca_{2.3}Cu_3O_y$ were found to be 482.5 KJ/mol, and the frequency factor, β, was $3.15 \times 10^{32}\ s^{-1}$.

Figure 9(a) shows an SEM micrograph of a full cross section of glass rod (≈2 mm diam and 25 mm long), indicating three distinct regions. Region A is the edge of the sample; region B appears to be the central part of the sample, with large black particles; and region C is similar to A (the outer edge of the sample), but black particles appear to be embedded in the matrix. The other end of the rod (sample) (Fig. 9b) shows the same microstructure, and Fig. 9(c) shows the central portion of the cross-sectional area of the other end of the rod.

The difference in the microstructure at the edge and center of the rod as shown in Fig. 9 may be due to the difference in the cooling rate during quenching. The XRD patterns also confirmed that the main crystalline phase in the interior of the bulk was $Bi_2Sr_2CaCu_2O_x$, but at the surface the phase appeared to be $Bi_2Sr_2CuO_x$. It could therefore be concluded that the formation mechanism in the interior of the rod was different from that at its surface and that the crystallization mechanism was affected

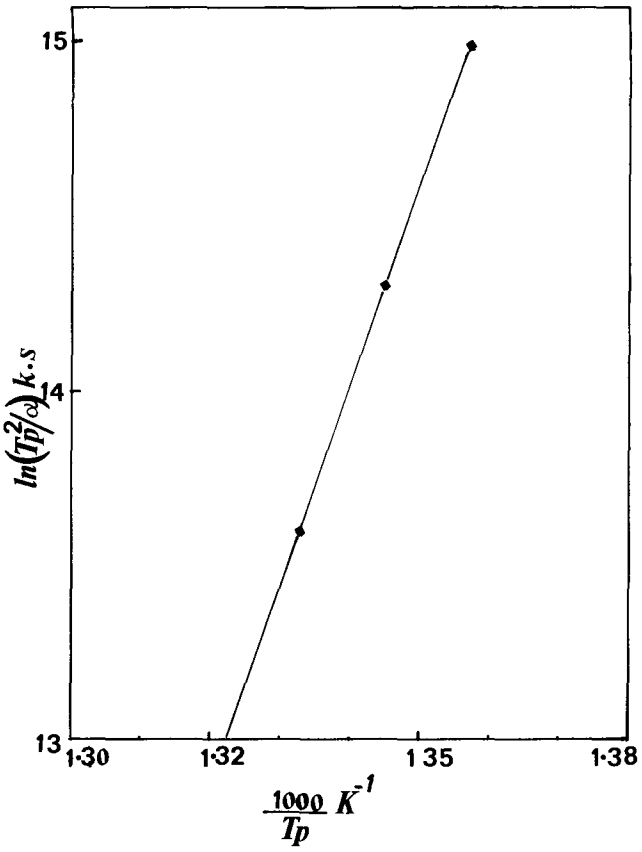

Fig. 8 Plot of $\ln(T_p^2/\alpha)$ versus reciprocal of peak maximum temperature for the crystallization of $(Bi_{1.6}Pb_{0.4})Sr_{1.7}Ca_{2.3}Cu_3O_y$ glass. The line is a linear least-squares fit to the data

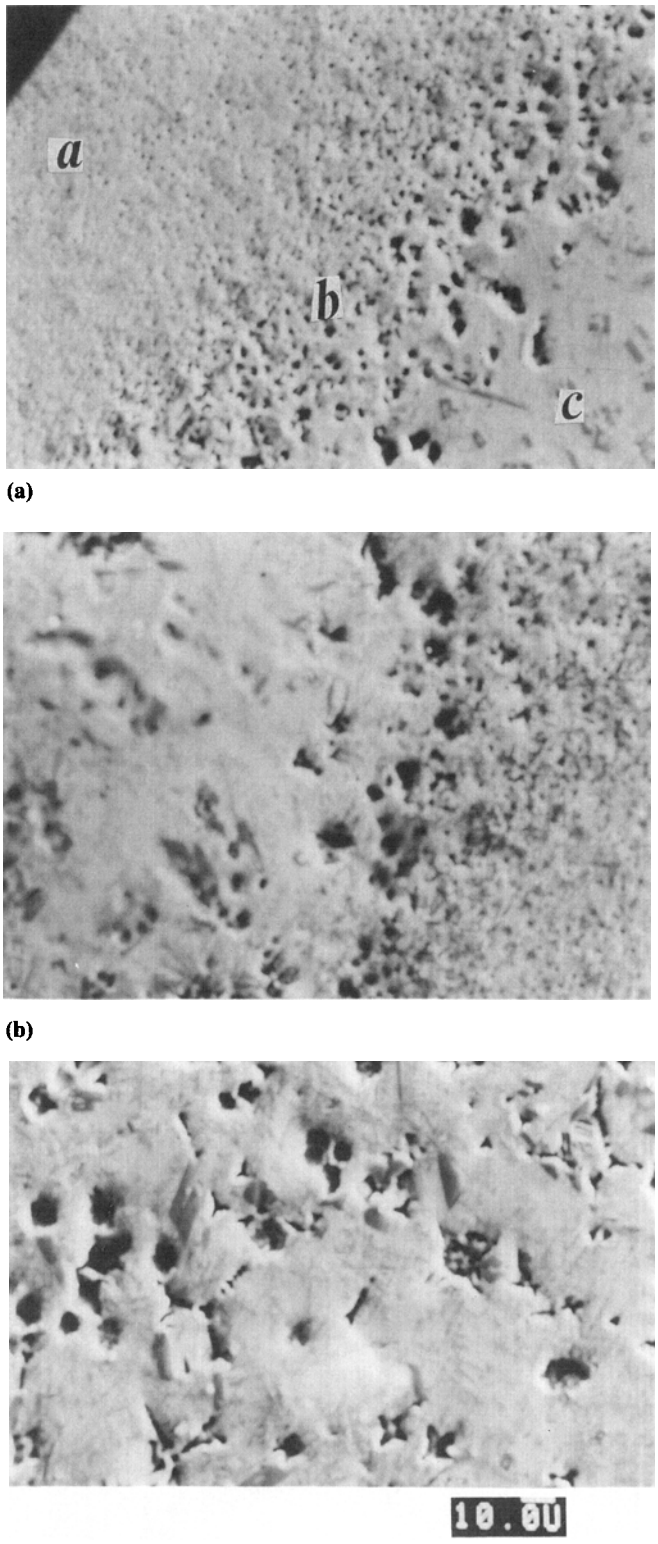

(a)

(b)

(c)

Fig. 9 SEM micrographs (400×). (a) Full cross section of the $(Bi_{1.6}Pb_{0.4})Sr_{1.7}Ca_{2.3}Cu_3O_y$ glass rod. (b) Other end of the glass rod. (c) Central portion of cross-sectional area of the glass rod

by oxygen diffusion into the sample during quenching. These results are consistent with our earlier results (Ref 11, 12).

4. Conclusions

We have confirmed that polycrystalline superconducting ceramic rods can be prepared by the glass-crystallization route. By rapidly cooling the melt, and insulating nonsuperconductive, metastable amorphous solid can be obtained. Heat treatment above the glass transition temperature of 494 °C results in the partial formation of the superconducting 2212 phase. The transformation kinetics are rapid, suggesting correlations in the short-range structure of the glass and in the periodic structure of the superconducting phase. The superconducting glass ceramic rods obtained by reheating glass rods at 850 °C for more than 120 h have a T_c ($R = 0$) of 105 K, whereas the disk specimens obtained by reheating the powdered glass compacts in the same way do not exhibit superconductivity above 85 K.

Acknowledgment

The support funded by the University of Bahrain is gratefully acknowledged.

References

1. D.G. Hinks, L. Soderholm, D.W. Capone II, B. Dabrowsi, A.W. Mitchell, and D. Shi, Preparation of Bi-Sr-Ca-Cu-O Superconductors from Oxide Glass Precursors, *J. Appl. Phys. Lett.*, Vol 53, 1988, p 423
2. T. Komatsu, R. Sato, K. Imai, K. Matsusita, and T. Yamashita, Effects of Annealing Conditions on Superconducting Properties of $BiCaSrCu_2O_x$ Ceramics Prepared by the Melt Quenching Method, *J. Appl. Phys.*, Vol 27, 1988, p L550
3. T. Minami, Y. Akamutsu, M. Tatsumisago, N. Tohge, and Y. Kowada, Glass Formation of High-T_c Compound $BiCaSrCu_2O_x$ by Rapid Quenching, *J. Appl. Phys.*, Vol 27, 1988, p L777
4. H.W. Zandberger, Y.K. Huang, M.J.V. Menken, J.N. Li, K. Kadowaki, A.A. Menovsky, G. Van Tendeloo, and S. Amelincks, Electron Microscopy on the T_c: 110 (Mid Point) Phase in System Bi_2O_3-SrO-CaO-CuO, *Nature*, Vol 332, 1988, p 620
5. H. Maeda, Y. Tanaka, M. Fukutomi, and T. Asano, A New High-T_c Oxide Superconductor without Rare-Earth Element, *J. Appl. Phys. Lett.*, Vol 27, 1988, p L209
6. R.M. Hazen, C.T. Prewitt, R.G. Angel, N.L. Roy, L.W. Finger, C.G. Hadidiacos, D.R. Veblen, P.J. Heaney, P.H. Hor, R.L. Meng, Y.Y. Sun, Y.Q. Wang, Y.Y. Xua, Z.J. Huang, L. Gao, J. Bechtold, and C.W. Chu, Superconductivity in the Very High-T_c Bi-Ca-Sr-Cu System Phase Identification, *Phys. Rev. Lett.*, Vol 60, 1988, p 1174
7. J.B. Torrance, Y. Tokura, S.J. Laplaca, T.C. Huang, R.J. Savoy, and A.I. Nazzal, New Class of High-T_c Structures, Intergrowth of Multiple Copper Oxide Perovskite, *Solid State Commun.*, Vol 66, 1988, p 703
8. H. Yinnon and D.R. Uhlmann, Applications of Thermoanalytical Techniques to the Study of Crystallization Kinetics in Glass Forming Liquids, *J. Non-Cryst. Solids*, Vol 54, 1983, p 253
9. M. Avrami, Kinetics of Phase Change, *J. Chem. Phys.*, Vol 7, 1939, p 1103
10. N.P. Bansal and R.H. Doremus, Determination of Reaction Kinetic Parameters from Variable Temperature DSC or DTA, *J. Thermal Anal.*, Vol 29, 1984, p 115
11. M.N. Khan, S. Al-Dallal, and A. Memon, Processing, Structure and Superconducting Properties of New High-T_c Superconductors from Oxide Glasses, *Proc. 3rd. Int. Symp. Advanced Materials* (Islamabad, Pakistan), Vol 196, 1993, p 20-24
12. M.N. Khan, A. Memon, S. Al-Dallal, M. Al-Othman, M. Zein, and W. Alnaser, The Influence of Pb, Ni and V Doping on the Characteristics of High-T_c Bi-Sr-Ca-Cu-O Superconductors, *Mod. Phys. Lett.*, Vol 7 (No. 26), 1993, p 1687